SPE · AAPG · SEG
CCUS
Carbon Capture, Utilization, and Storage

CCUS: 4443541

Forecasting CO_2 Plume Evolution for Geological Carbon Storage in Vertically Layered Deep Saline Aquifers Using Layer-Aware CNN-LSTM-FiLM Surrogate

Oluwatobi Akinyede*[1], Oluwasanmi Talabi[1], Siddharth Misra[1], 1. Texas A&M University, College Station, TX, United States.

This paper was prepared for presentation at the Carbon Capture, Utilization, and Storage conference held in The Woodlands, TX, 30 March – 01 April.

Abstract

Accurate forecasting of CO_2 plume evolution is critical for safe and effective geological carbon storage in deep saline aquifers. Plume migration is strongly controlled by vertically stacked stratigraphy and layer-scale permeability contrasts, yet resolving these effects with high-fidelity simulators remains computationally expensive. This study develops a layer-aware deep-learning surrogate for rapid prediction of CO_2 plume geometry during injection and post-injection periods. High-fidelity compositional simulations were generated using depth-dependent reservoir properties, multiple stratigraphic stacking regimes, and fixed-rate injection scenarios spanning 10–30 years followed by 50 years of monitoring. Layer-wise plume diameter trajectories were extracted as supervised targets. A one-dimensional convolutional–recurrent architecture with feature-wise linear modulation (CNN–LSTM–FiLM), augmented with a proper orthogonal decomposition (POD-aux) regularization, was trained to forecast plume evolution across depth and time. The surrogate accurately reproduces layer-controlled plume spreading while achieving approximately three orders of magnitude reduction in computational cost relative to full-physics simulation, enabling efficient scenario evaluation for geological carbon storage.

Introduction

Deep saline aquifers, typically located at depths greater than 800 m depth, are primary candidates for geological carbon storage due to their availability, capacity, confinement, and ability to maintain CO_2 in a supercritical state. Reliable forecasting of CO_2 plume migration is essential for managing pressure buildup, evaluating trapping behavior, and supporting storage monitoring. In stratified formations, plume evolution is governed by the vertical arrangement of permeable and low-permeability layers, which controls buoyant segregation and lateral spreading (Silin et al. 2008; Wen and Benson 2019). High-fidelity compositional simulators provide detailed representations of these processes but are computationally intensive, limiting their use in uncertainty analysis and rapid scenario screening (Zhang et al. 2026; Li and Yue 2025; Ghanbari et al. 2006; Nghiem et al. 2004). To overcome this limitation, data-driven surrogate models have emerged as efficient alternatives for plume forecasting. Prior work has demonstrated deep-learning-based prediction of plume migration, trapping efficiency, and generalization across operational conditions using recurrent networks and neural operators (Ren et al., 2024; Ren et al., 2025; Talabi et al., 2026; Falola et al., 2025a,b; Nunez et al., 2025). However, many existing approaches rely on simplified stratigraphic representations and do not explicitly encode layer ordering. Our current work addresses this gap by developing a layer-aware surrogate architecture that directly models vertically ordered stratigraphy and predicts layer-resolved plume evolution in deep saline aquifers.

Method

High-fidelity CO_2 injection simulations were generated using CMG-GEM for deep saline aquifers with reservoir tops between approximately 900 and 1500 m subsea depth. Pressure and temperature followed hydrostatic and geothermal gradients, while salinity was sampled as a depth-dependent variable with controlled variability. Each realization comprised 58 stacked interior layers, bounded by impermeable confining layers at the top and bottom. Injection was performed through a single vertical well, perforated across six consecutive near-base storage layers (starting layer sampled between layers 47–51 for each realization) at a constant rate per realization. Injection duration ranged from 10 to 30 years, followed by at least 50 years of post-injection monitoring or longer for cases with shorter injection period. For all cases, a total of 80 years injection and monitoring period was implemented. Figure 1 below shows a summary of our realization-level and per layer level input parameter ranges that were sampled for our dataset generation. It also shows the 5th, 50th and 95th percentiles selected at 6 months, 1 year, 5years and 10 years, illustrating the variability learned by the surrogate.

a)

Category	Parameter	Range / Definition
Reservoir geometry	Reservoir top depth	900–1500 m subsea
	Reservoir thickness	100–600 m
Petrophysical properties	Porosity (ϕ)	0.15–0.30
	Horizontal permeability (k_h)	20–650 mD
	Vertical anisotropy (k_v/k_h)	0.01–0.20
	Rock compressibility	4×10^{-7} – 4×10^{-5} kPa^{-1}
Initial conditions	Pressure	Hydrostatic gradient: 10.516 kPa/m
	Temperature	Geothermal gradient: 25 °C/km
	Salinity	30,000–80,000 ppm (depth-dependent)
Injection design	Injection well	Single vertical injector
	Base injection rate	1 Mt CO_2/year
	Injection rate (sampled)	Scaled from base case
	Injection period	10–30 years
	Monitoring period	50 years
Vertical structure	Number of storage layers	58
	Layer stacking regimes	Randomized, AR(1)-correlated, blocky run-length
Target definition	Plume metric	Layer-wise plume diameter
	Target range	0–7200 m

b)

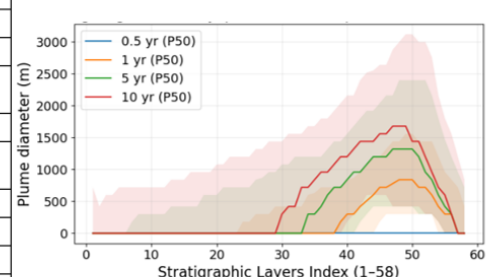

Figure 1. Dataset design and target variability (a) Summary of reservoir, petrophysical, and operational parameters used to generate simulation scenarios, including sampling ranges and fixed modeling assumptions, (b) Training-target variability shown as layer-wise plume diameter percentiles (P5–P50–P95) at selected times (0.5, 1, 5, and 10 years), illustrating the diversity of plume shapes learned by the surrogate across layered reservoir

Vertical layering was generated using three stacking methods designed to span realistic stratigraphic variability and edge cases for modelling stress-test as shown in Figure 2 below. These methods are: (i) randomized stacking, (ii) correlated autoregressive (AR(1)-type) stacking, and (iii) blocky run-length stacking including low-permeability intervals. Layer properties were sampled from sand-quality-dependent ranges for porosity, permeability, anisotropy, and compressibility. Multiphase flow behavior was diversified by assigning each sand-quality class a family of admissible relative permeability and capillary pressure values covering a range of scenarios possible per sand.

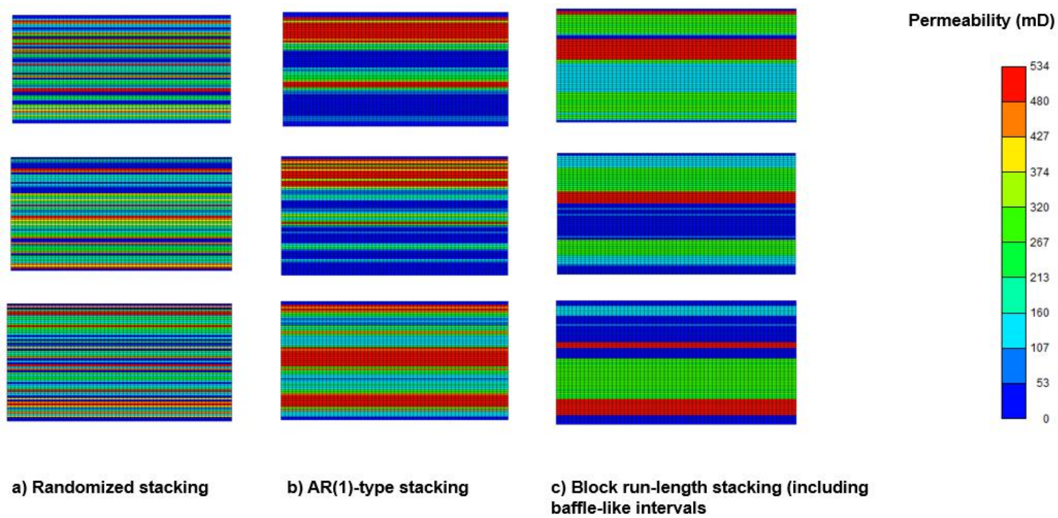

Figure 2. Representative layered stacking regimes. Example permeability fields for three realizations from each stacking regime: randomized stacking, correlated AR(1)-type stacking, and block run-length stacking including baffle-like intervals. Colors indicate horizontal permeability (mD). Axes and grid indices are omitted for clarity, emphasizing vertical layer organization rather than spatial scale.

The supervised learning target was defined as the layer-wise CO_2 plume diameter as a function of time, extracted from simulated saturation fields using a consistent plume threshold. This yields a target tensor spanning time and depth. Model inputs comprised three components namely (1) realization-level descriptors (e.g., depth, thickness, injection design), (2) a layer-resolved stratigraphic feature matrix, and (3) a time-dependent injection control sequence. Surrogate modeling employed a one-dimensional convolutional–recurrent architecture. A 1D convolutional neural network (CNN) encodes vertically ordered stratigraphy, a multilayer perceptron encodes realization-level descriptors, and feature-wise linear modulation (FiLM) conditions stratigraphic features on case-specific properties. A long short-term memory (LSTM) module propagates temporal information from injection controls. The fused representations are mapped through a linear head to predict plume diameter for all layers and times. A Proper Orthogonal Decomposition-based auxiliary (POD-aux) regularization term encourages consistency with dominant plume modes and improves generalization.

Results

Figure 3 demonstrates the surrogate's ability to reproduce plume geometry for three held-out test realizations. Figure 3a shows the layered saline aquifer structure for the selected test cases, highlighting permeability contrasts that govern buoyancy-driven migration and lateral spreading. Figure 3b presents plume overlay snapshots at 10, 30, 50, and 80 years for the same realizations. Across all time steps, the surrogate accurately reproduces plume shape, vertical extent, and lateral spread predicted by the high-fidelity simulation. Differences between predicted and simulated plume boundaries are generally confined to within one lateral grid block on either side of the plume front. Prediction accuracy was quantified using mean absolute error (MAE) in plume diameter relative to grid resolution. With a lateral grid-block size of 120 m, a tolerance of $\leq$ 240 m was adopted.

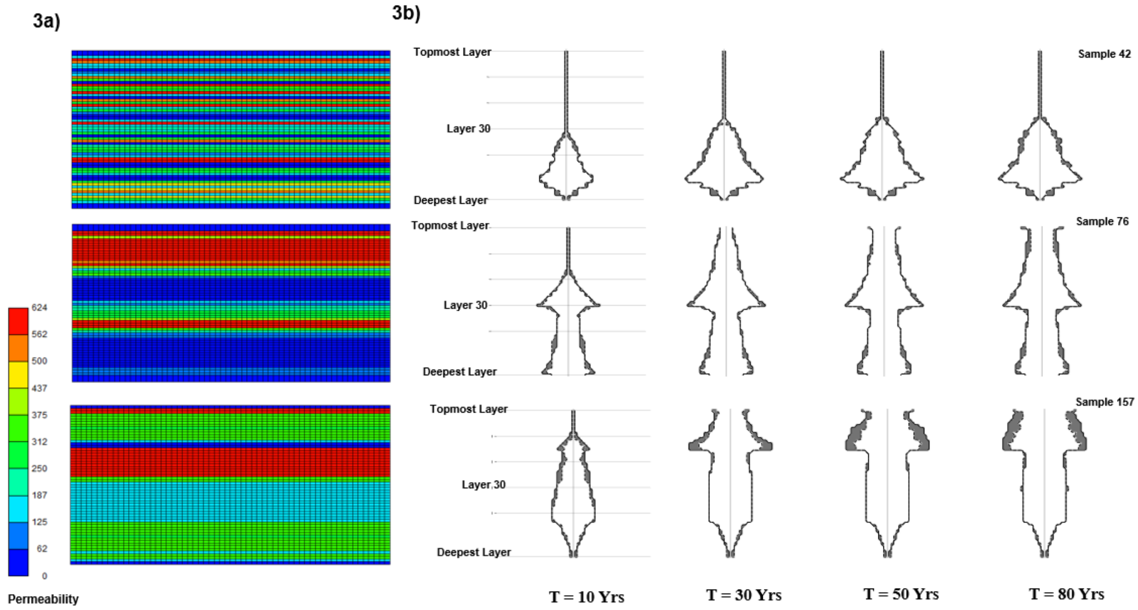

Figure 3. Visual comparison of simulated and surrogate-predicted plume geometry for a held-out test realization (a) Layered saline aquifer structure shown as a 2D slice colored by permeability, (b) 2D reconstructed plume geometry overlays at 10, 30, 50, and 80 years for the same realization. Solid black contours denote high-fidelity CMG simulation results, dashed black contours denote surrogate predictions, and gray regions indicate the spatial difference between the two outlines.

Across 300 held-out test realizations, the POD-aux-regularized surrogate achieved average errors well within this tolerance (< 179 m), corresponding to approximately 1.5 grid blocks. Once trained, surrogate inference required milliseconds per realization, compared with approximately one hour per scenario for full-physics simulation. This represents a computational speedup of approximately 1.4×10^3, enabling rapid evaluation of plume evolution over injection and post-injection periods.

Discussion

Accurate plume prediction is achieved by explicitly encoding vertical layer ordering within the surrogate. The convolutional encoder captures local correlations along depth that fully connected encoders failed to represent. FiLM conditioning incorporates realization-level variability without collapsing layer-specific effects, while POD-aux regularization stabilizes training and preserves physically meaningful plume structure. Alternative approaches, including purely reduced-order POD surrogates and autoencoder-based models, exhibited higher test errors exceeding grid-scale tolerance and reduced robustness.

Conclusions

This study presents a layer-aware CNN–LSTM–FiLM surrogate for forecasting CO_2 plume evolution in deep saline aquifers. Trained on dataset generated from high-fidelity simulations spanning multiple stratigraphic stacking regimes, the surrogate predicts layer-wise plume diameter with test errors below ≤240 m(within our grid tolerance) and achieves approximately three orders of magnitude reduction in computational cost relative to full-physics simulation. The results demonstrate that explicitly encoding vertically ordered stratigraphy is critical for accurate plume forecasting. The proposed methodology supports rapid scenario evaluation, uncertainty screening, and efficient assessment of plume behavior during injection and post-injection phases of geological carbon storage.

References

Falola, Y., Misra, S., and Nunez, A. 2024. "Integrating Neural Operators and Transfer Learning for Efficient Carbon Storage Forecasting." Paper presented at the ADIPEC, Abu Dhabi, UAE, November.

https://doi.org/10.2118/222406-MS.

Falola, Y., Misra, S., and Nunez, A. 2025a. Transfer Learning for Geological Carbon Storage Forecasting Using Neural Operator. Advances in Water Resources 199: 104948. https://doi.org/10.1016/j.advwatres.2025.104948.

Falola, Y., Misra, S., and Nunez, A. 2025b. "Geological and Engineering Insights from Transfer Learning with Fourier Neural Operators: A Case Study of CO_2 Storage Forecasting in Disparate Saline Aquifers." Applied Soft Computing 178: 113272. https://doi.org/10.1016/j.asoc.2025.113272.

Falola, Y., Misra, S., and Nunez, A. 2026. "Leveraging Transfer Learning for Reliable CO_2 Storage Forecasting across Diverse Operational Conditions." Fuel 403: 135990.

https://doi.org/10.1016/j.fuel.2025.135990.

Ghanbari, S., Al-Zaabi, Y., Pickup, G.E., Mackay, E., Gozalpour, F., and Todd, A.C. 2006. Simulation of CO_2 storage in saline aquifers. Chem. Eng. Res. Des. 84 (9): 764–775. https://doi.org/10.1205/cherd06007.

Kumar, V., Ren, G., Talabi, O., Misra, S., Odi, U., Silver, A., Gupta, A., and Temizel, C. 2024. "Geological Carbon Storage in Saline Aquifers: Factors Governing Residual and Solubility Trapping." Paper presented at the ADIPEC, Abu Dhabi, UAE, November.

https://doi.org/10.2118/222767-MS.

Li, X., and Yue, G. 2025. CO_2 trapping mechanism in deep saline aquifers under the control of composite geological factors. J. Supercrit. Fluids 221: 106547. https://doi.org/10.1016/j.supflu.2025.106547.

Nghiem, L., Sammon, P., Grabenstetter, J., and Ohkuma, H. 2004. Modeling CO_2 storage in aquifers with a fully coupled geochemical EOS compositional simulator. Paper presented at the SPE/DOE Symposium on Improved Oil Recovery, Tulsa, Oklahoma. SPE-89474-MS. https://doi.org/10.2118/89474-MS.

Ren, G., Talabi, O., Kumar, V., Misra, S., Odi, U., Silver, A., and Gupta, A. 2025. Trapped and Movable CO_2 in Geologic Carbon Storage: Deep-Learning Forecasting and Generalization Study. Paper presented at the International Petroleum Technology Conference (IPTC), Kuala Lumpur, Malaysia, February.

https://doi.org/10.2523/IPTC-24804-MS.

Ren, G., Talabi, O., Kumar, V., Misra, S., Odi, U., Silver, A., Gupta, A., and Temizel, C. 2024. Rapid Forecasting of Trapped and Movable Carbon Dioxide in Saline Aquifers Using LSTM-Based Sequence-to-Sequence Learning. Paper presented at the ADIPEC, Abu Dhabi, UAE, November.

https://doi.org/10.2118/222364-MS.

Silin, D., Patzek, T., and Benson, S.M. 2008. A modeling of buoyant gas plume migration. LBNL-1552E. Lawrence Berkeley National Laboratory.

Talabi, O., Ren, G., and Misra, S. 2026. AI-Driven Rapid Forecasting of CO_2 Plume Migration and Trapping Efficiency in Geological Carbon Storage. International Journal of Greenhouse Gas Control 149: 104535. https://doi.org/10.1016/j.ijggc.2025.104535.

Wen, G., and Benson, S.M. 2019. CO_2 plume migration and dissolution in layered reservoirs. Int. J. Greenh. Gas Control 87: 66–79. https://doi.org/10.1016/j.ijggc.2019.05.012.

Zhang, L., Zhang, S., Shan, L., and Yang, W. 2026. Effect of layered heterogeneity in saline aquifers on geological CO_2 storage. Fuel 408: 137765. https://doi.org/10.1016/j.fuel.2025.137765.